Chemical Engineering Science 109 (2014) 111–122

Contents lists available at ScienceDirect

Chemical Engineering Science

journal homepage: www.elsevier.com/locate/ces

# Liquefaction of wood in hot compressed water Part 1 — Experimental results

M. Mosteiro-Romero [a], F. Vogel [a,b,*], A. Wokaun [a]

[a] General Energy Research Department, Paul Scherrer Institut, 5232 Villigen PSI, Switzerland
[b] Institute for Biomass and Resource Efficiency, University of Applied Sciences Northwestern Switzerland, 5210 Windisch, Switzerland

## HIGHLIGHTS

- We studied the liquefaction of wood particles of different sizes in a batch reactor.
- Hydrothermal conditions always led to more liquid products than pyrolysis.
- At lower temperatures, the products of hydrolysis were mostly water-soluble.
- The obtained water-soluble products were stable products, not reacting any further.
- Small spherical particles were found on the surface of the charred wood.

## GRAPHICAL ABSTRACT

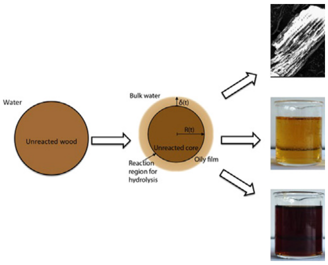

## ARTICLE INFO

*Article history:*
Received 4 September 2013
Received in revised form
17 December 2013
Accepted 23 December 2013
Available online 9 January 2014

*Keywords:*
Wood
Hot compressed water
Dissolution
Modeling
Fuel

## ABSTRACT

The dissolution of wood in subcritical water in the context of a hydrothermal biomass gasification process is studied in order to provide insight into the effects of the operating parameters during the liquefaction step on the product distribution. Batch experiments were conducted at temperatures of 250–350 °C and pressures of 15–30 MPa and at various holding times. The product yields showed that the early product-forming reactions are very fast, and to go to completion within the heating stage for the experimental setup used. A hydrolysis experiment using the water-soluble products as feedstock confirmed the obtained water-soluble products to be final, as they did not undergo further hydrolysis to other products. The conversion of wood to liquid and gaseous products as well as the carbon content of the solid residue increased with increasing temperature. At lower temperatures, the reaction products of hydrolysis were mostly water-soluble, while with increasing temperature the methanol-soluble products were most abundant. The hexane-soluble products were negligible in almost all cases, and the gas products were predominantly composed of $CO_2$. The experiments provide information about the yields of different products at different temperatures, their composition, and the effect of the operating conditions on the formation of primary and secondary char and on the limitations imposed on the primary product formation.

© 2014 Elsevier Ltd. All rights reserved.

## 1. Introduction

The hydrothermal treatment of wood is of interest to a variety of processes, such as hydrothermal gasification (HTG) to gaseous fuels, hydrothermal liquefaction (HTL) to liquid fuels, wood liquefaction to produce chemicals and hydrothermal carbonization (HTC). Under these conditions, the special properties of water

---

[*] Corresponding author at: General Energy Research Department, Paul Scherrer Institut, 5232 Villigen PSI, Switzerland.
*E-mail address:* frederic.vogel@psi.ch (F. Vogel).

0009-2509/$ - see front matter © 2014 Elsevier Ltd. All rights reserved.
http://dx.doi.org/10.1016/j.ces.2013.12.038

around the critical point allow water to be simultaneously used as the reaction medium, as a solvent, as a reactant and as a catalyst in some of the reactions. In the first three processes, the goal is to liquefy the feedstock in the initial preheating step, producing light organic compounds that can be easily catalytically converted to gaseous products, upgraded to liquid fuels or converted to other chemicals, whereas in the latter the goal is to produce high energy density char.

Under ideal HTG and HTL conditions, the feedstock is completely liquefied in the initial step. In practice, however, the operational parameters can cause the feedstock to be converted incompletely, producing undesirable products like heavy tars and char that cannot be converted in the subsequent step. These losses lower the conversion efficiency of the process, and can also cause blockages by solid or tar accumulation and hinder the operation of a plant. Thus, it is desirable to find the ideal operating parameters for the preheater in order to maximize the yield of the desired liquefaction products.

The liquefaction of wood was studied through a series of batch experiments within the context of a hydrothermal gasification process (Vogel et al., 2007). However, the findings of this work are also of interest to the other types of processes for hydrothermal treatment of wood. The results of these experiments were subsequently used to develop a mathematical model, presented in a separate publication (Mosteiro-Romero et al., in this issue).

A summary of previous work on the uncatalyzed dissolution of wood under hydrothermal conditions is presented in Table 1. The results show a large spread due to the different methodologies used as well as the large amounts of error often found in the mass balances. In general, the holding temperature appears to have the largest effect on the conversion of wood. The type of reactor used does neither show a strong effect on the conversion nor on the product distribution. Furthermore, the feed concentration does not show a strong correlation with the conversion.

Wood is a feedstock of variable characteristics, given that properties such as its composition, porosity and density can change significantly between samples. Due to the uncertainty such variations create, model compounds are often used both for experimental work as well as for the development of hydrolysis models. Typical wood plants consist of approximately 40–50% cellulose, 20–30% hemicellulose, 20–28% lignin and trace amounts of other substances (Yu et al., 2008). As the most abundant component in woody biomass, cellulose is most often used as a model compound for hydrolysis studies in order to reduce the variability of the feedstock properties between experiments. As the study of cellulose hydrolysis alone cannot capture the complexity of wood degradation however, actual wood decomposition was studied here. For this purpose, samples of the coniferous tree spruce were used as the raw material for all experiments.

Under the conditions of interest for biomass liquefaction, wood is mainly decomposed through two pathways: pyrolysis and hydrolysis. The predominance of either one of these pathways over the other depends strongly on the operating conditions.

Hydrolysis reactions are those in which bonds are broken by reaction with water. In the hydrolysis of wood, the water-insoluble constituents (cellulose, hemicellulose and lignin) are converted to smaller, water-soluble compounds by depolymerization. It is a surface reaction, since water needs to come into contact with the biomass in order to react, and it is acid-catalyzed. A full overview of the liquefaction process and its reaction pathways at subcritical conditions can be found in an article by Toor et al. (2011).

Pyrolysis is a thermal conversion process that involves the degradation of organic material by the application of heat in the absence of oxidizing agents to produce volatile compounds (oils and gas) and char. It is used for the conversion of biomass to fuel but, as with any thermal conversion process, its conversion efficiency depends strongly on the moisture content of the feedstock. The conversion of wood to fuels and char through pyrolysis is a well-studied process, a good overview of which can be found in a review paper by Di Blasi (2008). A study including both hydrolysis and pyrolysis conditions for the same wood samples and their modeling is not available in the literature.

A series of batch experiments was conducted at different temperatures (250–350 °C) and holding times (0, 10 and 20 min) under both hydrolysis and pyrolysis conditions. While for hydrolysis experiments the wood was treated with water at pressures of approximately 25 MPa, for pyrolysis experiments the wood was dried and treated under the same conditions in the absence of water and oxygen but in the presence of argon. Additional experiments were carried out to test the effects of particle size and pressure.

## 2. Materials and methods

### 2.1. Materials

The raw material used for all experiments was spruce wood, which was milled in a knife mill and screened in a vibratory sieve (400–800 μm mesh). The moisture content of the feedstock was 12.6% on average. For the pyrolysis experiments, the wooden particles were additionally dried at 105 °C in a vacuum oven beforehand.

Additional experiments were carried out in order to study the effects of particle size on the reaction kinetics. For these, special approximately spherical particles of diameters 0.4–0.5 mm and 0.9–1 mm were prepared. Ultrapure water was used for all hydrolysis experiments, and the reactor was pressurized using argon gas (purity $\geq 99.998\%$).

### 2.2. Experimental setup

A two-part experimental setup was used, comprising a heated section in which the reaction was carried out and an unheated section for safety and control. A simplified schematic of the experimental setup is shown in Fig. 1.

The experiments were carried out in an unstirred stainless steel tubular microreactor system manufactured by *HiP, USA*, with inner dimensions of 30.48 cm in length and 1.43 cm in diameter (internal volume ~49 mL). The reactor was fit with a K-type thermocouple (diameter 1.59 mm) at the bottom. During experiments, the heated section was lowered into a preheated fluidized sand bath (type SBL-2D, manufactured by *Techne, UK*). The reactor was connected to the cold section by a capillary of 229 mm in length and 1 mm internal diameter. The unheated section comprised a pressure transducer and two valves in a row (also manufactured by *HiP*) for gas withdrawal and addition before and after each experiment. The system was connected to a computer, which recorded, at two-second intervals, the reactor temperature and pressure, as well as the temperature of the sandbath and in the surrounding environment.

### 2.3. Experimental procedure

At the beginning of each hydrolysis experiment, a sample of wooden particles was weighed and placed in the reactor. Ultrapure water was then added in a ratio of 10 g of water per g of dry wood. The amount of water added to the reactor was adjusted to account for the moisture content in the wood in order to maintain the aforementioned ratio. For pyrolysis experiments, oven-dried wood was used, and no other substances were added to the reactor. The

**Table 1**
Experimental results for the hydrolysis experiments carried out in this work compared to published results for the uncatalyzed hydrothermal liquefaction of wood.

| Ref. | Wood type | Particle size (mm) | Reactor type | HR (K/min) | $T_{hold}$ (°C) | $t_{hold}$ (min) | $p_{hold}$ (MPa) | Feed (g wood/L water) | Solid residue (wt%) | Liquid products (wt%) | | Gas products (wt%) |
|---|---|---|---|---|---|---|---|---|---|---|---|---|
| | | | | | | | | | | SS | WS | |
| Modell (1985) | Maple | 3x0.5 | S | N/A | 377 | 5–60 | ~22.1 | 1.1–3.7$^{a}$ | 0 | N/A | N/A | 17–39.5$^{a}$ |
| Goudriaan and Peferoen (1990) | Bioshell slurry | 0.1 | T | > 60 | 350 | 6 | 18 | 149 | 42.5 | | 39.5 | 18 |
| Minowa et al. (1994) | Bark chips | < 1 | N/A | 9 | 302 | 0–10 | 10 | 67 | 15–45 | 20–45 | | N/A |
| Qu et al. (2003) | Cunninghamia | < 0.2 | S | 4–6 | 280–360 | 10–30 | N/A | 80–125 | 26–40 | 7–24 | 6–16 | N/A |
| Karagöz et al. (2004) | Sawdust | N/A | S | 3 | 180–280 | 15–60 | N/A | 167 | 41–73 | 4–8 | 21–45 | 2–14 |
| Zhong and Wei (2004) | Chinese pine | < 0.2 | S | 4–6 | 280–360 | 10 | N/A | 80 | 23–28 | 17–21 | 9–16 | N/A |
| Zhong and Wei (2004) | Chinese poplar | < 0.2 | S | 4–6 | 280–360 | 10 | N/A | 80 | 19–24 | 18–26 | 9–17 | N/A |
| Zhong and Wei (2004) | Chinese oak | < 0.2 | S | 4–6 | 280–360 | 10 | N/A | 80 | 14–15 | 25–31 | 9–17 | N/A |
| Hashaikeh et al. (2007) | Willow | N/A | SC | N/A | 215–230 | 25 | 10 | 154 | 35–37 | N/A | N/A | N/A |
| | | N/A | SC | N/A | 300 | 25 | 10 | 154 | 48 | N/A | N/A | N/A |
| | | N/A | B | 17 | 450 | 0 | N/A | N/A | 40–60 | N/A | N/A | N/A |
| Bhaskar et al. (2008) | Cherry | N/A | S | 3 | 280 | 15 | N/A | 167 | 31 | 16 | 34 | 20 |
| Bhaskar et al. (2008) | Cypress | N/A | S | 3 | 280 | 15 | N/A | 167 | 44 | 8 | 39 | 10 |
| Xu and Lad (2008) | Jack pine | < 0.8 | B | N/A | 300–380 | 5–60 | N/A | 100 | 21–40 | 23–40 | 5–17 | N/A |
| Zhang et al. (2008) | Pretreated aspen | 1.3–2.5 | B | 5–14 | 350 | 10 | 20 | 111 | 14–25 | 50–62 | | 24–25 |
| | | | | 140 | | | | | 6–7 | 72–74 | | 20–21 |
| Yáñez et al. (2009) | Wattle | < 8 | B | N/A | 170–240 | 0 | N/A | 125 | 55–93 | 7–28 | | 0–26 |
| Cheng et al. (2010) | Pine | 0.8 | S | 10 | 300 | 15 | N/A | 100 | 30 | 40 | 24 | 6 |
| Knežević et al. (2010) | Sawdust | 0.2 | B | 139 | 350 | 3–58 | 17 | 37 | 12–22 | 45–58 | | 11–16 |
| | | | | | | | | | 15–30$^{a}$ | 53–76$^{a}$ | | 7–11$^{a}$ |
| Sun et al. (2010) | Paulownia | < 0.2 | B | 5 | 280–360 | 10 | N/A | 167 | 19–23 | 19–27 | 10–17 | 10–17 |
| Yan et al. (2010) | Loblolly pine | 0.6–1.2 | B | N/A | 200–260 | 5 | 1.6–5 | 200 | 63–83 | 13–15 | | 9–20 |
| Liu et al. (2012) | Cypress | < 0.4 | S | 4 | 180–300 | 0 | ≤ 13 | 100 | 36–86 | 2–15 | 27–51 | 1–9 |
| | | | | | 260 | 0–40 | | 100 | 33–36 | 12–15 | 43–49 | 6–8.5 |
| | | | | | 260 | 0 | | 83–250 | 36–49 | 5–15 | 40–48 | 5–8 |
| Waldner (2007) | Spruce | ~0.3 | B | 36 | 240 | 120 | 30 | 111 | N/A | 13$^{a}$ | | 5$^{a}$ |
| Waldner (2007) | Spruce | | | 30–55 | 300–350 | 0–21 | 30 | 111 | N/A | 29–56$^{a}$ | | 4–11$^{a}$ |
| This work | Spruce | 0.4–0.8 | B | 14–36 | 250–350 | 0–20 | 17–30 | 100 | 23–57$^{a}$ | 16–38$^{a}$ | 13–30$^{a}$ | 1–7$^{a}$ |

N/A, not available; HR, heating rate; $T_{hold}$, holding temperature; $t_{hold}$, holding time; SS, organic solvent-soluble products; WS, water-soluble products; B, batch reactor; S, stirred batch reactor; SC, semi-continuous reactor; and T, tubular continuous reactor.

[a] Mass determined on a carbon basis.

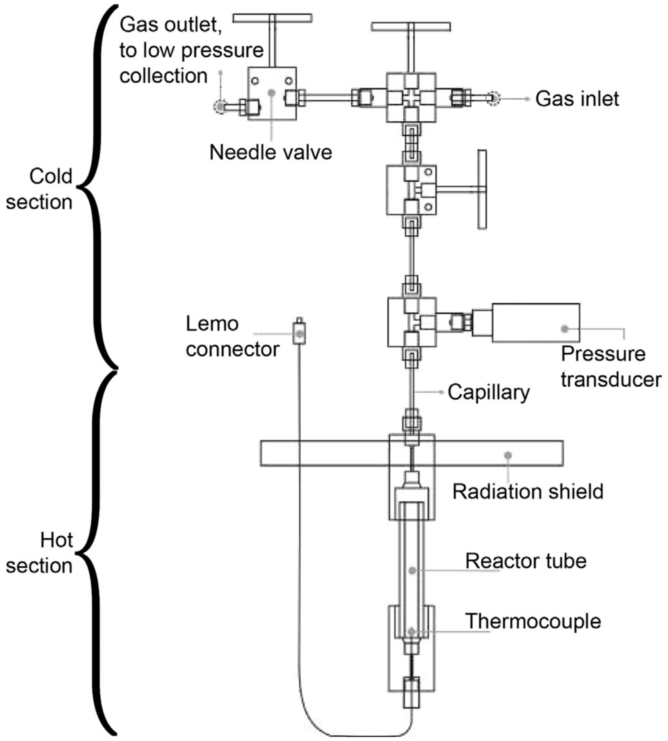

**Fig. 1.** Batch reactor setup used for the experiments. Adapted from Waldner and Vogel (2005).

reactor was closed with a 280 Nm torque wrench. The system was then evacuated and subsequently filled with argon as inert gas. This procedure was repeated three times in order to remove any other gases in the reactor, which was finally pressurized with inert gas. Given that the holding pressure cannot be adjusted during the course of the experiment, the Ar pressure in the reactor before heating was adjusted between 4 and 13 MPa, depending on the amount of water in the reactor and the holding temperature, in order to achieve the desired holding pressure of 24–26 MPa. In addition to maintaining the required pressure conditions for each experiment, the inert gas served as a means to check for gas leakage during the experiment.

The reactor was then lowered into the fluidized sand bath, which was preheated to about 20 °C above the desired holding temperature and covered with a sheet of metal, which served as a radiation shield for the system. The heating time for the experiments was between 7 and 13 min (typically 9–10 min), regardless of the holding temperature. Typical heating rates were thus 20–35 K $\text{min}^{-1}$, which in the pyrolysis case corresponds to the slow pyrolysis regime. Once the reactor temperature reached the predefined holding time, the sand bath temperature and air flow rate were regulated during the holding period in order to maintain the holding temperature close to the target value. Once the predefined holding time was reached, the reactor was removed from the sand bath and immediately quenched in a water bath for fast cooling.

For the retrieval of the products from the reactor, the extraction method described by Müller and Vogel (2012) was followed. First, after the reactor cooled down to ambient temperature, the gas content was removed by connecting a 3 or 10 L gas bag (manufactured by *SKC, USA*) to the valve outlet and opening both valves. Since the reactor was highly pressurized, the gases were almost completely removed from the reactor. The reactor was then opened and the contents were poured into a separating funnel. Subsequently, the reactor was flushed repeatedly with water, which was then added to the separating funnel to remove the water-soluble reaction products (WSP). The procedure was then repeated with hexane to remove the non-polar reaction products remaining on the reactor walls (hexane-soluble products, HSP). The water and hexane phases were stirred in the separating funnel to ensure the removal of all water- and hexane-soluble products present in the original reactor contents and on the solid residue's surface. The two phases were then separated in the funnel and filtered in vacuum through a membrane filter (manufactured by *Schleicher & Schuell, Germany*, particle retention in liquid $< 2\ \mu\text{m}$).

In order to remove the remaining tars, the reactor was flushed repeatedly with methanol, poured into the separating funnel and finally filtered through the same filter containing the solid residue in order to recover any water- and hexane-insoluble products remaining on these surfaces (methanol-soluble products, MSP).

The remaining solid residue (SR) on the filter is composed of primary and secondary char. We define primary char as the solid residue from the initial biomass, which mostly retains its original structure. Secondary char, on the other hand, is formed by repolymerization of liquefaction products, and thus bears no structural resemblance to the unreacted biomass.

### 2.4. Analyses

The composition of the gas phase was analyzed by gas chromatography (GC) immediately after the experiment with an *HP* 6890 *GC* for Ar, $CO_2$, $CH_4$, CO and $H_2$ content. No hydrogen was detected for any of the experiments. The total volume of the gas obtained from the reaction was determined by a 1-L graduated syringe (*Hamilton S*-1000).

The carbon content in the solid and liquid phases was determined by total carbon analysis with an *Elementar VarioTOC Cube*. The reaction products were then grouped according to their separation phase, that is, they were analyzed as either Solid Residue (SR), Water-Soluble Products (WSP), Hexane-Soluble Products (HSP), Methanol-Soluble Products (MSP) or Gaseous products (G). The yields of the products in each of these phases are defined on a carbon mass basis, that is, for each product the yield *Y* is

$$Y_i = \frac{m_{C,i}}{m_{C,feed}} \tag{1}$$

In addition to the amount of carbon, it is also of interest to identify the typical compounds found in each product phase. Therefore, the methanol and hexane phases were analyzed by gas chromatography–mass spectrometry (GC–MS) in an *HP* 6890 *series* gas chromatograph coupled to a mass spectrometer (*HP* 5973 *mass selective detector*). No method was available to resolve the mixture of organics in the water phase.

The particle size distribution of the feedstock and the solid residue samples was measured in a *Horiba LA-950* analyzer. For each sample of solid residue, at least three measurements were performed. In addition, the same number of measurements was performed after 1 min of ultrasonic treatment in order to separate any aggregates in the sample. Due to the high complexity involved in measuring particles of different shapes, the particle size analyzer (PSA) assumes all particles to be spherical. The particles produced by milling are, however, not spherical but needle-shaped, and the size of the sieved wood used as feedstock varied widely, often exceeding the maximum mesh size used in the longitudinal direction. Nonetheless, this measurement at least gave an estimate of the average decrease in particle size under different reaction conditions. In order to obtain better insight into the properties of the solid residue from experiments under different conditions and to study the primary and secondary char formation in wood hydrolysis, selected samples were imaged by scanning electron microscopy (SEM).

## 3. Results and discussion

A total of 29 experiments using sieved milled wood, at both hydrolysis and pyrolysis conditions, were carried out at temperatures of 250–350 °C, pressures of 24–26 MPa and holding times of 0, 10 and 20 min. These are discussed in Sections 3.1–3.5. In addition, hydrolysis experiments were carried out using larger particle sizes (0.4–0.5 cm and 0.9–1.0 cm) and water-soluble products recovered from a previous experiment as the feedstock. These are discussed in Sections 3.6 and 3.7. The experimental conditions and the product yields of all experiments are given in the Appendix.

### 3.1. Carbon balance

The carbon balance closure for the experiments was between 80% and 100%. Müller (2012) quantified the influence of the different potential sources of error in experiments performed with this setup and found the most important to be the quantitative removal of the sticky tars and solids from the wall of the reactor. This explains the increasing error with increasing temperature and holding time. From this consideration, only experiments in which the error was less than or equal to 10% were considered, except for experiments at 350 °C or holding times of 20 min, for which a 15% error in the carbon balance was allowed.

### 3.2. Product yields

The product yields in each phase for the selected experiments under hydrolysis and pyrolysis conditions are shown graphically in Figs. 2 and 3. Under all conditions, hydrolysis experiments produced significantly more liquid products, as well as a lower amount of solid residue. In both cases the amount of solid residue left in the particle at the end of the experiment decreased with temperature, while the formation of the products increased. The measured amount of hexane-soluble products (HSP) was negligible under all experimental conditions except for pyrolysis at 350 °C.

The repeatability of our experiments was assessed by performing selected experiments multiple times. For pyrolysis experiments, the results were highly reproducible. For hydrolysis experiments, the gas composition and the carbon content of the solid residue were generally reproducible, whereas the variation in the yields of the liquid products was generally higher. We expect these deviations to be mainly caused by losses in the experimental work-up procedure.

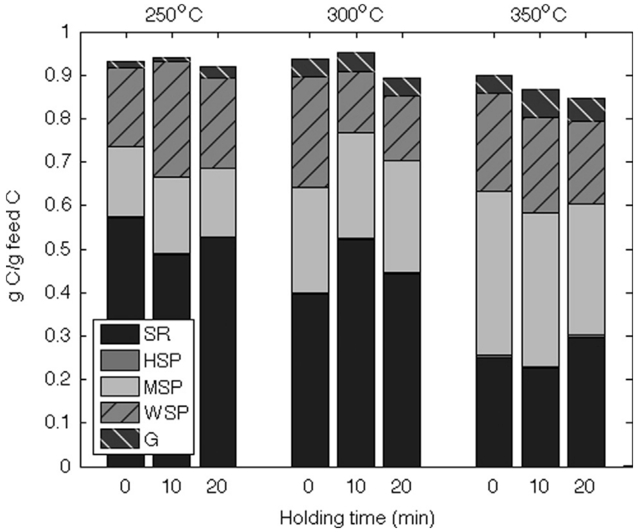

**Fig. 2.** Experimental results from selected hydrolysis experiments using small particles (400–800 μm sieve). Target experimental conditions were 250–350 °C and 25 MPa, and holding times were 0, 10 and 20 min. SR, solid residue; HSP, hexane-soluble products; MSP, methanol-soluble products; WSP, water-soluble products; and G, gaseous products.

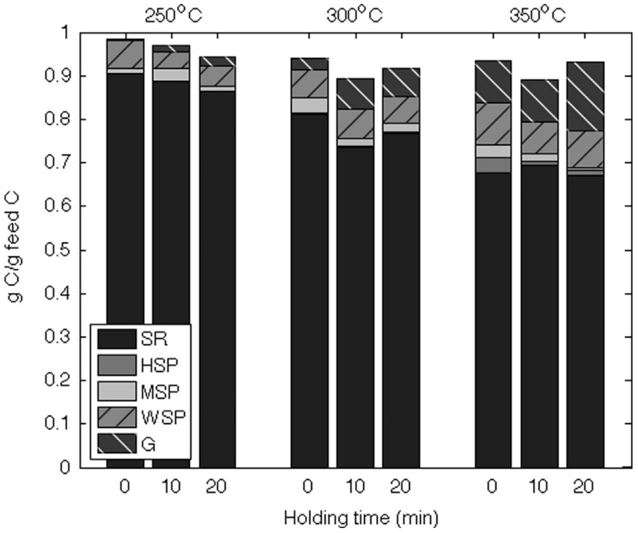

**Fig. 3.** Experimental results from selected pyrolysis experiments using small particles (400–800 μm sieve, dried, no water). Target experimental conditions were 250–350 °C and 25 MPa, and holding times were 0, 10 and 20 min.

The yields obtained in this work are compared to published results in Table 1. The majority of the work found in the literature used smaller particles and operated at much lower heating rates. Nonetheless, some works (Zhong and Wei, 2004; Sun et al., 2010) obtained substantially lower solid residue yields while operating at similar temperatures, however the yields of liquid products were also smaller in these experiments. The fastest heating rate was achieved by Knežević et al. (2010), who used small capillaries as reactors, and Zhang et al. (2008), who used an induction heating system. The product distribution for the former's experiments is fairly similar to the experimental results from this paper at the same temperature (350 °C), although the holding time played a much larger role in their work, as the results for longer experiments show much higher conversions than shorter ones. Zhang et al.'s results, on the other hand, show a much higher conversion to products, and particularly gaseous products, at the same holding temperature. The results from Waldner and Vogel (2005) using the same setup show a comparable yield of liquid products, although the gas yield was also greater.

In spite of the different holding times used, however, the formation of products at each temperature did not show a strong dependence on the holding time, and the variability in the measured yields for all experiments at each temperature was in the range of the measurement error. From the experimental data, it appears that the heating times for the reactor setup to reach the holding temperature (in the range of 9–10 min for most experiments) were so long that all product-forming reactions reached completion within the heating stage, and thus changing the subsequent holding time had no effect on the yields of the products for the milled wood experiments. This is in agreement with the findings of Hashaikeh et al. (2007), who found that increasing the temperature from 215 to 300 °C did not affect the dissolution time. One notable exception was the gas yield under pyrolysis conditions, which increased with increasing holding time.

In general, however, no kinetic information could be extracted for the product yields under hydrolysis and pyrolysis conditions with

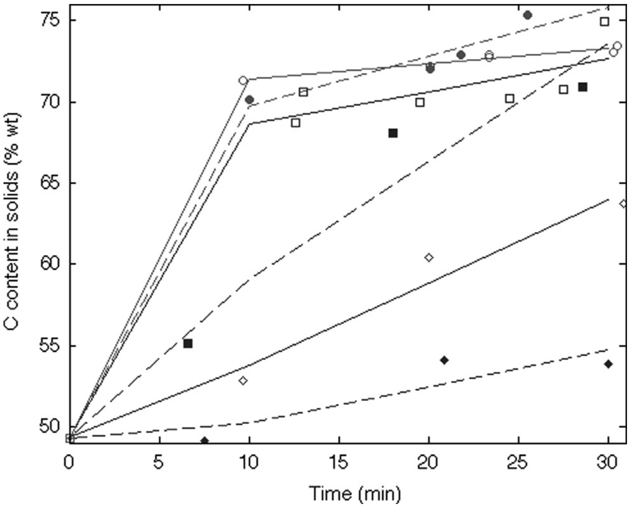

**Fig. 4.** Carbon content in the solid residue at different temperatures and holding times with linear fits for hydrolysis (solid line) and pyrolysis (dashed line) at 250 °C (◇: hydrolysis; ◆: pyrolysis), 300 °C (□: hydrolysis; ■: pyrolysis) and 350 °C (○: hydrolysis; ●: pyrolysis).

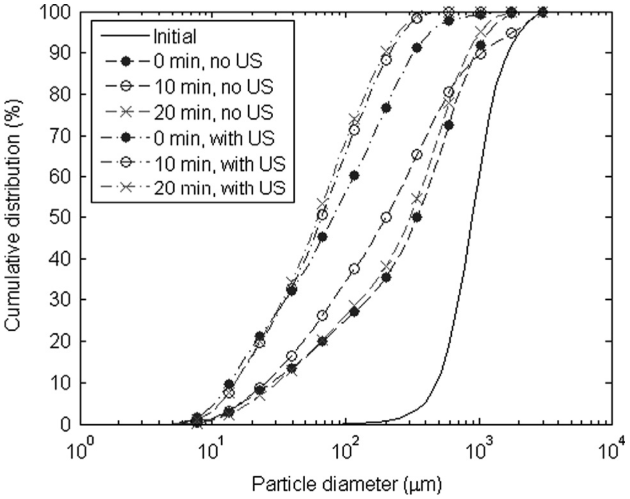

**Fig. 5.** Cumulative particle size distribution $Q_3$ of milled spruce samples before hydrothermal treatment and solid residue samples from hydrolysis experiments at 300 °C and holding times of 0, 10 and 20 min without ultrasonic treatment (solid line, labeled "no US") and after 1 min of ultrasonic treatment (dashed line, labeled "with US").

the reactor setup used. This was not true, however, of the charring of the particle. The carbon content of the solid residue under the different operating conditions at different holding times is shown in Fig. 4. While all of the other reactions have been assumed to have proceeded to completion during the heating stage, the carbon content in the particle continued to increase with increasing holding time. Therefore, it appears that charring reactions continue to proceed even after the other reactions have stopped.

### 3.3. Solid residue characterization

For the hydrolysis case, the particle size distribution was measured for samples at different holding temperatures and times, both with and without ultrasonic treatment. As described by Kobayashi et al. (2009), particle aggregates were found in the solid residue sample. The ultrasonic vibration is applied in order to eliminate such aggregates and to give a more accurate measurement of the actual particle size.

The cumulative particle size distribution of the solid residue from hydrolysis experiments at different temperatures and holding times is shown in Fig. 5. The ultrasonic treatment has a noticeable effect on the measured particle size distributions, as less large particles were detected under all conditions and the distribution became broader due to the aggregates being separated into smaller particles of different sizes. This is shown by the large decrease in the 50% particle diameter of the solid residue for the experiments, which was between 270 and 350 µm for the experiments with a holding time of 0 min without ultrasonic treatment, whereas after ultrasonic treatment it was approximately 70–90 µm. The 50% particle diameter of the milled wood was about 890 µm, and thus the median size after hydrolysis was approximately one order of magnitude smaller than the raw wood, which is a greater decrease than the one reported by Kobayashi et al. (2009) (1/7 of the original particle size) for experiments at different temperatures with a heat up time of 20 min and a 1 min holding time. In general terms, the particle size distribution did not show a strong dependence on the holding time, which is in agreement with the observed lack of additional product formation with increasing holding time.

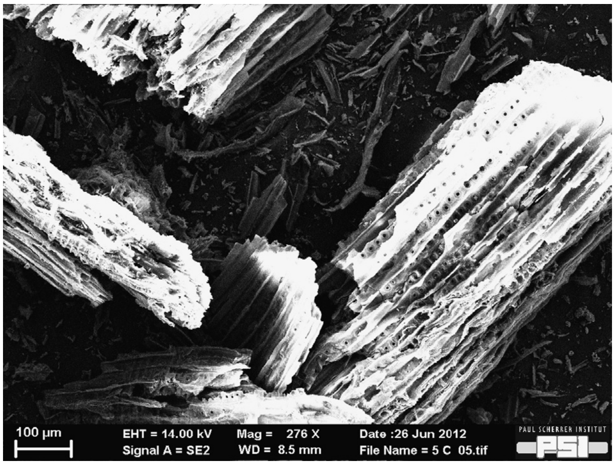

**Fig. 6.** SEM micrograph of a SR sample taken from a hydrolysis experiment at 350 °C and holding time of 10 min.

In order to provide further insight into the structure of the solid residue and the formation of secondary char in the experiments, samples from the high temperature experiments at different holding times were analyzed by SEM. The solid residue was mostly composed of material presenting a structure similar to that of the raw wood, as seen in Fig. 6. In addition, smaller amounts of secondary char, formed by the repolymerization of liquefaction products, were found in the sample. The secondary char was composed of small spherical particles with diameters up to approximately 6 µm (Fig. 7). These were generally found as either individual spheres or in aggregates of several spherical particles, but generally not on the wooden structure's surface. Thus, it appears that secondary char is formed completely separately from the primary char, and that the primary products are free to leave the particle surface. Secondary char was found in all samples, and none of the experimental conditions exhibited a higher propensity to form secondary char, *i.e.*, increasing holding time did not cause more secondary char to form under the conditions studied.

### 3.4. Product characterization

In order to identify the chemical compounds contained in the MSP and HSP, selected samples for both pyrolysis and hydrolysis were analyzed by GC–MS. Surprisingly, while the abundance of

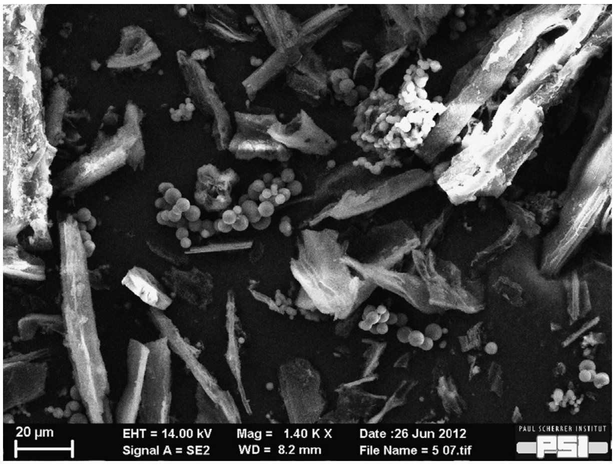

**Fig. 7.** SEM micrograph of a SR sample taken from a hydrolysis experiment at 350 °C and holding time of 10 min showing spherical particles formed.

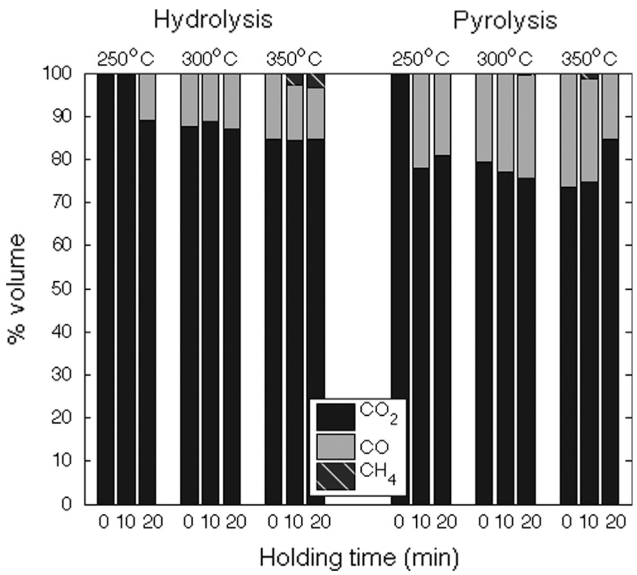

**Fig. 8.** Gas composition of selected hydrolysis and pyrolysis experiments. Target experimental conditions were 250–350 °C and 25 MPa, and holding times were 0, 10 and 20 min.

products changed between samples, the larger peaks occurred at the same retention times in all cases, meaning that the most abundant compounds were the same for both phases. The peaks detected for each compound were then matched to a database, and the compounds were found to be: 2-methoxyphenol, also known as guaiacol (match quality: 90); 2-ethoxy-4-ethylphenol, or creosole (match quality: 94); 2-methoxy-4-ethylphenol, or 4-ethylguaiacol (match quality: 87); and 2′,4′-dihydroxy-propiophenone (match quality: 64). Given its low match quality and its noticeably different structure, the identification of the fourth peak is the least reliable.

The other three detected compounds are common products of thermochemical biomass decomposition. Guaiacol is a lignin monomer often used as a lignin model compound (Saisu et al., 2003; Pińkowska et al., 2012), and it is known to be one of the main products of lignin pyrolysis (Demirbaş, 2000). In lignin hydrolysis experiments, Pińkowska et al. (2012) found guaiacol to be one of the dominant products along with 4-methylguaiacol (at higher temperatures), while Saisu et al. (2003) detected both guaiacol and ethylguaiacol amongst many substituted guaiacols in the products. In addition, Zhang et al. (2008) detected all three compounds in the products of hydrothermal liquefaction of aspen wood chips pretreated with sulfuric acid to remove partial hemicellulose.

The composition of the gas products of each experiment was analyzed by GC, and the main compounds found in the gas phase of the experiments are shown in Fig. 8. In all cases, the gas phase was found to consist predominantly of carbon dioxide, and the remainder of the gas phase was generally composed of carbon monoxide. For the majority of the hydrolysis experiments, $CO_2$ accounted for 81–90% of the gaseous products, whereas the CO content was 10–16% in most cases. The formation of CO was generally higher than the results reported by Waldner (2007) (5–10 vol%), and it increased for longer residence times with increasing temperatures. In addition to these two main products, at high temperatures small amounts (3–4%) of $CH_4$ were also formed. For low temperature hydrolysis, increasing the holding time caused the yield of CO to increase.

Under pyrolysis conditions, the share of CO in the gaseous product was higher than for the hydrolysis case, accounting for

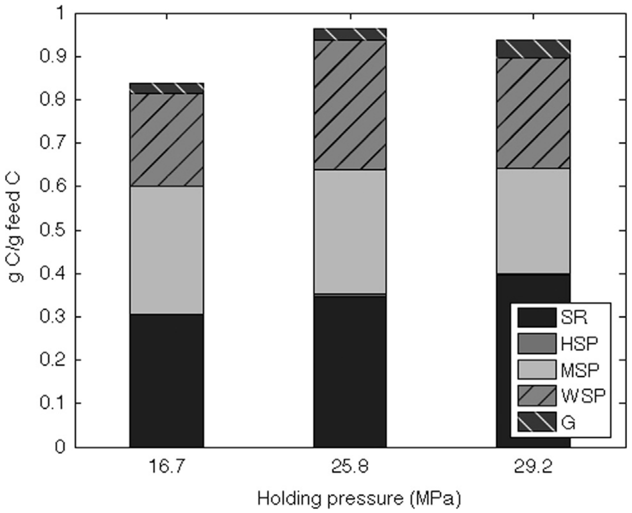

**Fig. 9.** Product distribution from hydrolysis experiments performed at different pressures, 300 °C, and no holding time.

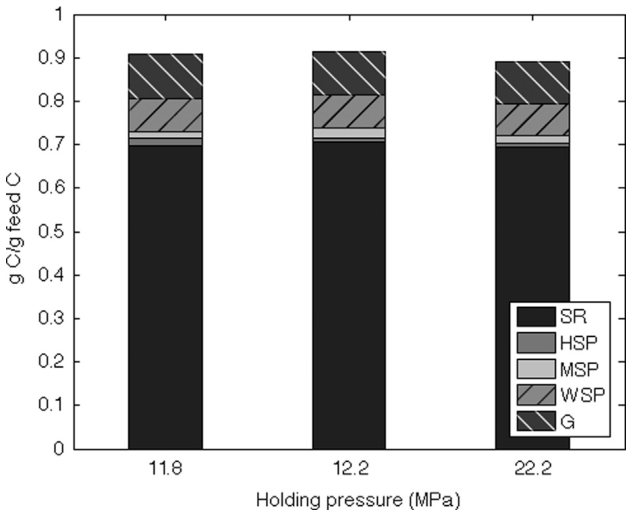

**Fig. 10.** Experimental results from pyrolysis experiments using small particles (400–800 µm sieve) at 350 °C and 10 min holding times at different pressures.

15–26% in most experiments. Regarding the share of CO in the gas products, the opposite relationship was seen for both lower and higher temperatures, while at 300 °C it was fairly constant for all holding times. Methane was only detected in one experiment, at 350 °C and 10 min holding time.

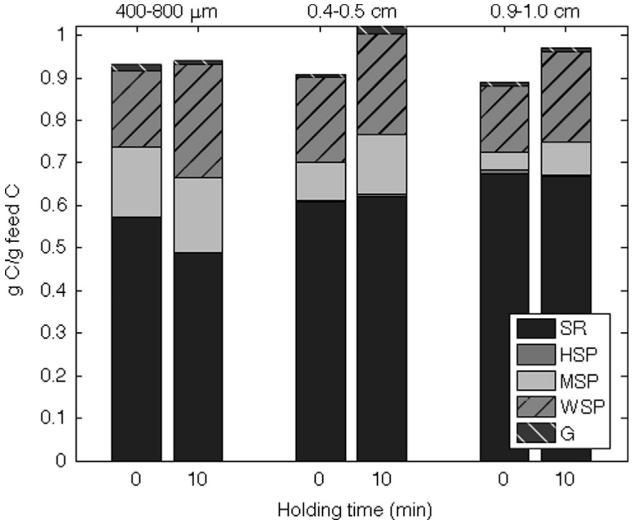

**Fig. 11.** Comparison of the experimental results from hydrolysis experiments using milled wood and wooden blocks. Target experimental conditions were 250 °C and 25 MPa.

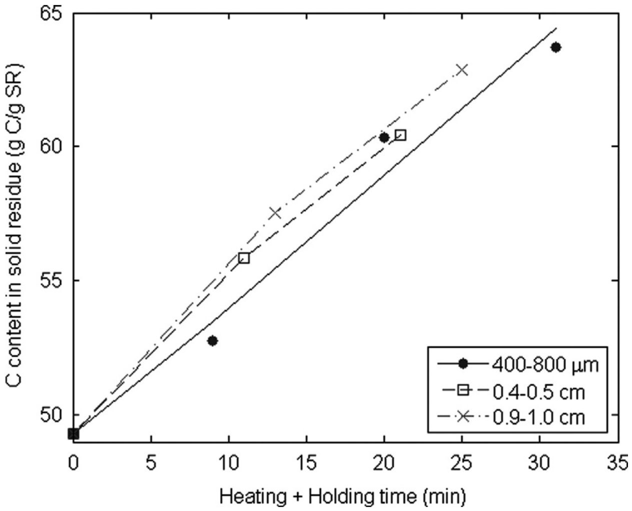

**Fig. 12.** Carbon content in the solid residue at different holding times for hydrolysis experiments with milled wood and 0.4–0.5 cm and 0.9–1.0 cm blocks, including linear fit for the smaller particle experiments.

### 3.5. *Pressure effects*

The temperature and pressure in the reactor were monitored throughout the experimental procedure. At the beginning of each experiment, the pressure is far higher than the saturation pressure due to the pressurization of the reactor with argon gas. As the temperature increases, the saturation pressure is approached, but never reached. Thus, for all hydrolysis experiments performed, the water remained in liquid form throughout the entire process, ensuring that hydrolysis conditions were maintained at all times.

The operating pressure is known to affect the hydrolysis reactions due to the changes in water properties it causes around the critical point. However, under the conditions of interest in this work, the pressure was not found to have a strong correlation with the product distribution, as shown in Fig. 9. For experiments performed at 300 °C, a holding time of 0 min and pressures of 17, 26 and 29 MPa, the changes in product composition are in the range of the error in the carbon balance.

Nonetheless, in order to ensure consistency in the experimental results, the pressure for the hydrolysis experiments was carefully maintained within the target range by adjusting the inert gas content in the reactor. For pyrolysis experiments, on the other

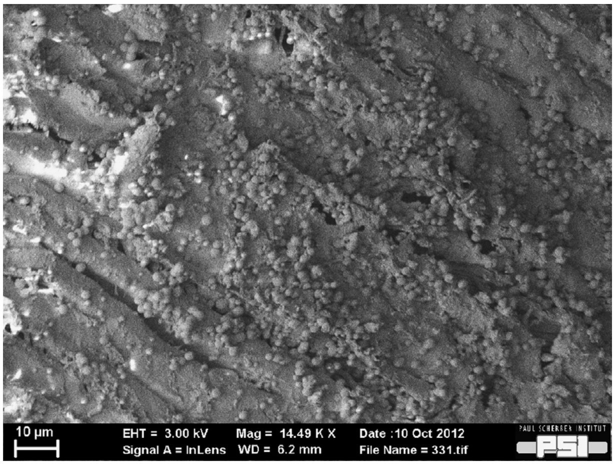

**Fig. 14.** SEM micrograph of a SR sample taken from a large particle (0.9–1.0 cm) hydrolysis experiment at 250 °C and holding time of 10 min showing spherical particle formation on the surface.

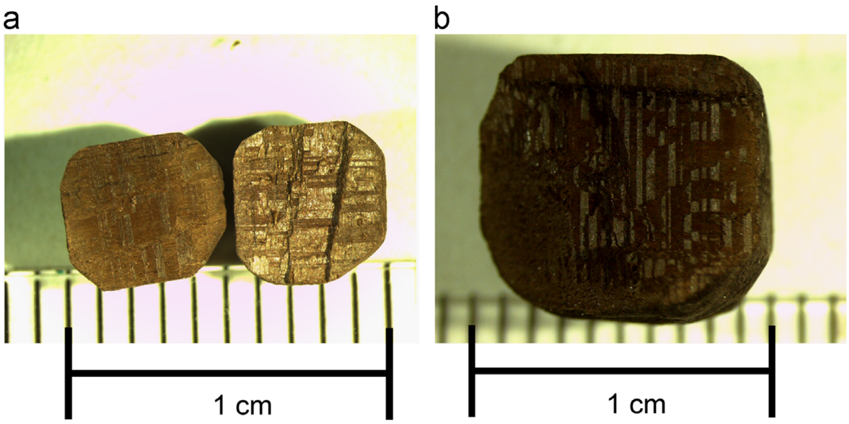

**Fig. 13.** Cross section of SR particles from the hydrolysis experiments using 0.4–0.5 cm (a) and 0.9–1.0 cm (b) blocks at 250 °C and holding time of 10 min.

hand, it was harder to maintain consistency in the pressure range by the same method, and therefore pyrolysis experiments often showed larger differences in the holding pressures. Thus, the reliability of results obtained from pyrolysis experiments at different pressures was also analyzed.

Fig. 10 shows the yields for the different phases for pyrolysis experiments conducted at holding temperatures of 350 °C and holding times of 10 min at pressures of around 12 and 22 MPa. The heating time was also approximately 10 min for the two latter experiments, while for the first experiment it was 18 min. The results, however, are nearly identical for all phases under all experimental conditions. Furthermore, the carbon content in the solid residue for all cases was between 72% and 73%, and the gas composition was approximately 75% $CO_2$ and 25% CO in all cases. Thus, under the experimental conditions investigated, the pressure does not affect the yields of pyrolysis products.

### 3.6. Large particle size experiments

Four more experiments were performed to test the effects of particle size on product yields.

The product yields in each phase for the large particle hydrolysis experiments are shown graphically and compared to the experiments carried out under the same conditions using milled wood (400–800 μm sieve) in Fig. 11. The results show an increase in the amount of solid residue left at the end of each experiment for larger particles. Increasing the holding time, however, appears to have no effect on the decomposition of the solid residue, and since the particles were much larger (an entire order of magnitude greater than the median diameter of the milled wood), SR losses are unlikely. Thus, the increase in the MSP and WSP yields with increasing holding time is most likely due to the higher losses in the lower holding time experiments rather than to the formation of additional products with increasing holding times. Thus, even for larger particle sizes the hydrolysis reactions appear to have gone to completion within the holding time. Interestingly, the WSP yield was similar in all cases (15.5–26.7% of feed C). As shown in Fig. 12, the rate of increase of the carbon content in the solid residue was approximately the same for all particle sizes. Furthermore, Fig. 13 shows that the interior of the particles after the experiments did not show gradients in the extent of charring. Thus, under the conditions studied, the charring reactions appear to occur homogeneously throughout the particle. This observation also suggests the absence of heat transfer limitations in the particles. Finally, the change in particle size was not as dramatic as in the smaller particle experiments, as the particle size was approximately the same before and after hydrothermal treatment.

The solid residue from the large particle experiments was also analyzed by SEM. The wooden surface appeared mostly unchanged in both cases. Spherical particles as those found for the small particle experiments were abundant in the long holding time experiment for particles of size 0.9–1.0 cm, shown in Fig. 14. These have been suggested to be secondary char formed by repolymerization of liquefaction products, as found for experiments using glycerol performed by Müller (2012), which might indicate that there were significant diffusion limitations for primary products leaving the reaction region for larger particle sizes. The formation of secondary char on the particle surface would also create a protective layer hindering further dissolution of the wood. However, other authors have suggested these spheres to be lignin that became liquid at the reaction temperatures and then resolidified at ambient temperature. This single experiment's result, however, does not present enough evidence to confirm either as a general conclusion.

### 3.7. Hydrolysis of water-soluble products

Since the product yields appear to indicate that the residence time had no effect on the formation of products (*i.e.*, all reactions went to completion within the heating stage), a further experiment was performed in order to test the stability of the water-soluble products. In this experiment, the aqueous phase obtained from a hydrolysis experiment performed at 350 °C and 10 min holding time was used as the feedstock and was further treated at 350 °C and 23.5 MPa during 10 min. The vast majority of the products of this experiment remained in the aqueous phase (87.7% of the feed C). 4.3% of the feed C was recovered as MSP, 2.4% as HSP and 2.7% in gaseous form. The amount of SR recovered was negligible ($<0.01\%$ of the feed C). The results of this experiment confirm the stability of the WSP obtained from hydrolysis, which supports the conclusion that the hydrolysis reactions had already gone to completion and that further extending the holding times would not have an effect on the product yields.

## 4. Conclusions

Wood hydrolysis and pyrolysis at the conditions of interest for a hydrothermal gasification process were analyzed through a series of batch experiments using milled spruce and spruce blocks. The product yields showed all reactions to have gone to completion within the heating stage. This was true of all experiments, including those specifically conducted to slow down the kinetics by lowering the reaction temperature and using larger particle sizes. Thus, it was concluded that early product-forming reactions in wood hydrolysis are very fast. This is in agreement with findings in the literature for cellulose hydrolysis (Cantero et al., 2013).

Nonetheless, the experiments did provide information about the yields of different products at different temperatures, their composition, and the effect of the operating conditions on the formation of primary and secondary char and on the limitations imposed on the primary product formation. The conversion of wood to liquid and gaseous products as well as the carbon content of the solid residue increased with increasing temperature. At lower temperatures, the reaction products of hydrolysis were mostly water-soluble, while with increasing temperature the methanol-soluble products were most abundant. The hexane-soluble products were negligible in almost all cases, and the gas products were predominantly composed of $CO_2$.

## Acknowledgments

The authors would like to thank the following people for their technical support: Thanh-Binh Truong, Hemma Zöhrer (TOC), Erich De Boni (SEM), Jörg Schneebeli (GC-MS) and Daniel Peitz (PSA).

## Appendix A. Full experimental results

### A.1. Hydrolysis experiments

Results from the small particle (400–800 μm sieve) hydrolysis experiments are given in Table A1.

**Table A1**
Results from the small particle (400–800 μm sieve) hydrolysis experiments.

| Experiment | Reactor inputs | | | Experimental conditions | | | | Product yields | | | | | | SR C content (wt%) |
|---|---|---|---|---|---|---|---|---|---|---|---|---|---|---|
| | $m_{wood}$ (g) | $m_{water}$ (g) | $p_{Ar}$ (MPa) | $T_{hold}$ (°C) | $p_{hold}$ (MPa) | $t_{heat}$ (min) | $t_{hold}$ (min) | SR | HSP | MSP | WSP | $G$ | Losses[a] | |
| | | | | | | | | % of feed C | | | | | | |
| H250-00 | 1.999 | 19.746 | 10.5 | 251 | 25.3 | 9 | 0 | 57.2 | 0.14 | 16.3 | 18.0 | 1.53 | 6.83 | 52.8 |
| H250-10 | 2.002 | 19.754 | 10.4 | 256 | 24.6 | 10 | 10 | 48.8 | 0.12 | 17.6 | 26.7 | 0.86 | 5.98 | 60.4 |
| H250-20 | 2.002 | 19.755 | 10.5 | 254 | 24.3 | 11 | 20 | 52.7 | 0.15 | 15.7 | 20.8 | 2.71 | 7.98 | 63.7 |
| H300-00-1 | 1.919 | 18.944 | 4.25 | 301 | 16.7 | 9 | 0 | 30.5 | 0.11 | 29.4 | 21.4 | 2.35 | 15.8 | 66.5 |
| H300-00-2 | 2.001 | 19.751 | 9.99 | 301 | 29.2 | 13 | 0 | 34.6 | 0.52 | 28.7 | 29.8 | 2.72 | 3.22 | 70.6 |
| H300-00-3 | 2.000 | 19.754 | 7.99 | 301 | 25.8 | 12 | 0 | 39.6 | 0.21 | 24.3 | 25.6 | 4.13 | 5.69 | 68.7 |
| H300-10-1 | 3.000 | 14.632 | 4.25 | 307 | 15.5 | 9 | 10 | 52.1 | 0.23 | 24.4 | 13.9 | 4.55 | 4.76 | 69.9 |
| H300-10-2 | 3.001 | 16.623 | 4.16 | 297 | 15.4 | 21 | 10 | 45.0 | 0.14 | 15.7 | 14.8 | 4.00 | 20.3 | 70.2 |
| H300-10-3 | 3.000 | 27.125 | 4.28 | 308 | 17.8 | 14 | 10 | 46.6 | 0.19 | 19.8 | 13.1 | 3.35 | 17.0 | 72.2 |
| H300-20-1 | 2.001 | 19.795 | 8.94 | 318 | 30.4 | 8 | 20 | 34.1 | 0.33 | 30.0 | 20.6 | 5.26 | 8.96 | 70.7 |
| H300-20-2 | 2.001 | 19.795 | 6.97 | 320 | 24.8 | 10 | 20 | 44.4 | 0.35 | 25.6 | 15.0 | 3.92 | 10.2 | 74.9 |
| H350-00 | 1.997 | 19.790 | 4.40 | 352 | 26.4 | 9 | 0 | 25.1 | 0.44 | 37.8 | 22.5 | 4.15 | 10.0 | 71.3 |
| H350-10-1 | 2.000 | 19.750 | 4.53 | 357 | 25.1 | 13 | 10 | 31.6 | 0.16 | 23.4 | 19.0 | 6.79 | 19.0 | 72.9 |
| H350-10-2 | 2.000 | 19.773 | 4.25 | 362 | 25.9 | 10 | 10 | 22.7 | 0.25 | 35.3 | 21.9 | 6.37 | 13.4 | 72.2 |
| H350-20-1 | 2.000 | 19.749 | 4.64 | 362 | 27.1 | 10 | 20 | 25.0 | 0.32 | 30.5 | 18.6 | 5.98 | 19.7 | 73.0 |
| H350-20-2 | 1.999 | 19.744 | 4.28 | 361 | 25.5 | 10 | 20 | 29.7 | 0.54 | 30.0 | 19.1 | 5.41 | 14.3 | 73.5 |

[a] Losses $= 100\% - \sum_i Y_i$.

## A.2. Pyrolysis experiments

Results from all pyrolysis experiments are given in Table A2.

**Table A2**
Results from all pyrolysis experiments.

| Experiment | Reactor inputs | | Experimental conditions | | | | Product yields | | | | | | SR C content (wt%) |
|---|---|---|---|---|---|---|---|---|---|---|---|---|---|
| | $m_{wood}$ (g) | $p_{Ar}$ (MPa) | $T_{hold}$ (°C) | $p_{hold}$ (MPa) | $t_{heat}$ (min) | $t_{hold}$ (min) | SR | HSP | MSP | WSP | $G$ | Losses[a] | |
| | | | | | | | % of feed C | | | | | | |
| P250-00 | 2.001 | 13.1 | 251 | 24.6 | 7 | 0 | 90.6 | 0.05 | 1.01 | 6.56 | 0.29 | 1.51 | 49.9 |
| P250-10 | 1.998 | 13.2 | 255 | 25.5 | 11 | 10 | 88.7 | 0.07 | 2.73 | 3.81 | 1.46 | 2.75 | 54.1 |
| P250-20 | 2.003 | 13.5 | 254 | 26.0 | 10 | 20 | 86.4 | 0.08 | 1.08 | 4.72 | 1.93 | 5.39 | 53.9 |
| P300-00 | 2.000 | 10.1 | 302 | 21.0 | 6 | 0 | 81.2 | 0.09 | 3.68 | 6.36 | 2.50 | 5.48 | 55.1 |
| P300-10 | 1.750 | 4.69 | 313 | 10.9 | 8 | 10 | 73.6 | 0.29 | 1.66 | 6.74 | 7.08 | 10.6 | 68.1 |
| P300-20 | 2.002 | 10.1 | 306 | 22.7 | 8 | 20 | 76.7 | 0.27 | 2.11 | 5.98 | 6.71 | 6.03 | 70.9 |
| P350-00 | 2.000 | [b] | [b] | [b] | [b] | 0 | 67.7 | 3.51 | 3.00 | 9.62 | 9.50 | 6.72 | 70.1 |
| P350-10-1 | 2.000 | 4.47 | 359 | 11.8 | 18 | 10 | 69.8 | 1.71 | 1.62 | 7.47 | 10.3 | 9.12 | 71.5 |
| P350-10-2 | 2.000 | 4.20 | 358 | 12.2 | 11 | 10 | 70.7 | 0.87 | 2.25 | 7.66 | 9.94 | 8.61 | 72.9 |
| P350-10-3 | 2.000 | 8.95 | 356 | 22.2 | 10 | 10 | 69.4 | 0.91 | 1.78 | 7.35 | 9.63 | 10.9 | 72.0 |
| P350-20 | 2.000 | 8.22 | 363 | 20.8 | 6 | 20 | 67.1 | 1.11 | 0.69 | 8.47 | 15.8 | 6.88 | 75.3 |

[a] Losses $= 100\% - \sum_i Y_i$.
[b] Reactor pressure and temperature data lost.

## A.3. WSP hydrolysis experiment

Results from the WSP hydrolysis experiment are given in Table A3.

**Table A3**
Results from the WSP hydrolysis experiment.

| Experiment | Reactor inputs | | | Experimental conditions | | | | Product yields | | | | | | WSP from experiment |
|---|---|---|---|---|---|---|---|---|---|---|---|---|---|---|
| | $m_{soln.}$ (g) | C content (mg C/g) | $p_{Ar}$ (MPa) | $T_{hold}$ (°C) | $p_{hold}$ (MPa) | $t_{heat}$ (min) | $t_{hold}$ (min) | SR | HSP | MSP | WSP | $G$ | Losses[a] | |
| | | | | | | | | % of feed C | | | | | | |
| H350-W | 20.1 | 3.498 | 4.50 | 359 | 23.4 | 11 | 10 | 0.01 | 2.4 | 4.3 | 87.7 | 2.7 | 3.0 | H350-10-2 |

[a] Losses $= 100\% - \sum_i Y_i$.

### A.4. Large particle hydrolysis experiments

Results from the large particle hydrolysis experiments are given in Table A4.

**Table A4**
Results from the large particle hydrolysis experiments.

| Experiment | Particle size (cm) | Reactor inputs | | | Experimental conditions | | | | Product yields | | | | | | SR C content (wt%) |
|---|---|---|---|---|---|---|---|---|---|---|---|---|---|---|---|
| | | $m_{wood}$ (g) | $m_{water}$ (g) | $p_{Ar}$ (MPa) | $T_{hold}$ (°C) | $p_{hold}$ (MPa) | $t_{heat}$ (min) | $t_{hold}$ (min) | SR | HSP | MSP | WSP | $G$ | Losses[a] | |
| | | | | | | | | | % of feed C | | | | | | |
| H250-00-k1 | 0.4–0.5 | 0.374 | 3.6987 | 12.2 | 251 | 24.2 | 11 | 0 | 60.8 | 0.51 | 8.89 | 19.9 | 0.86 | 9.10 | 55.9 |
| H250-10-k1 | 0.4–0.5 | 0.349 | 3.448 | 12.3 | 254 | 25.7 | 11 | 10 | 62.2 | 0.53 | 14.1 | 23.5 | 2.00 | −2.29 | 60.4 |
| H250-00-k2 | 0.9–1.0 | 0.495 | 4.888 | 11.8 | 251 | 23.8 | 13 | 0 | 67.4 | 0.86 | 4.18 | 15.5 | 0.93 | 11.1 | 57.5 |
| H250-10-k2 | 0.9–1.0 | 1.059 | 10.559 | 11.5 | 253 | 24.3 | 15 | 10 | 66.9 | 0.19 | 7.71 | 21.3 | 1.12 | 2.80 | 62.9 |

[a] $\text{Losses} = 100\% - \sum_i Y_i$.

### A.5. Gas composition of all experiments

Gas composition measured by gas chromatography for all experiments are given in Table A5.

**Table A5**
Gas composition measured by gas chromatography for all experiments.

| Experiment | Experimental conditions | | | Gas composition | | |
|---|---|---|---|---|---|---|
| | $T_{hold}$ (°C) | $p_{hold}$ (MPa) | $t_{hold}$ (min) | $CO_2$ | CO | $CH_4$ |
| | | | | vol (% ) | | |
| H250-00 | 251 | 25.3 | 0 | 100 | 0 | 0 |
| H250-10 | 256 | 24.6 | 10 | 100 | 0 | 0 |
| H250-20 | 254 | 24.3 | 20 | 89 | 11 | 0 |
| H300-00-1 | 301 | 16.7 | 0 | 86 | 14 | 0 |
| H300-00-2 | 301 | 29.2 | 0 | 86 | 14 | 0 |
| H300-00-3 | 301 | 25.8 | 0 | 89 | 11 | 0 |
| H300-10-1 | 307 | 15.5 | 10 | 89 | 11 | 0 |
| H300-10-2 | 297 | 15.4 | 10 | 90 | 10 | 0 |
| H300-10-3 | 308 | 17.8 | 10 | 89 | 11 | 0 |
| H300-20-1 | 318 | 30.4 | 20 | 87 | 13 | 0 |
| H300-20-2 | 320 | 24.8 | 20 | 87 | 13 | 0 |
| H350-00 | 352 | 26.4 | 0 | 85 | 15 | 0 |
| H350-10-1 | 357 | 25.1 | 10 | 84 | 13 | 3 |
| H350-10-2 | 362 | 25.9 | 10 | 81 | 16 | 3 |
| H350-20-1 | 362 | 27.1 | 20 | 84 | 12 | 4 |
| H350-20-2 | 361 | 25.5 | 20 | 85 | 12 | 3 |
| H350-W | 359 | 23.4 | 10 | 100 | 0 | 0 |
| H250-00-k1 | 251 | 24.2 | 0 | 100 | 0 | 0 |
| H250-10-k1 | 254 | 25.7 | 10 | 100 | 0 | 0 |
| H250-00-k2 | 251 | 23.8 | 0 | 100 | 0 | 0 |
| H250-10-k2 | 253 | 24.3 | 10 | 100 | 0 | 0 |
| P250-00 | 251 | 24.6 | 0 | 100 | 0 | 0 |
| P250-10 | 255 | 25.5 | 10 | 78 | 22 | 0 |
| P250-20 | 254 | 26.0 | 20 | 81 | 19 | 0 |
| P300-00 | 302 | 21.0 | 0 | 79 | 21 | 0 |
| P300-10 | 313 | 10.9 | 10 | 77 | 23 | 0 |
| P300-20 | 306 | 22.7 | 20 | 76 | 24 | 0 |
| P350-00 | [a] | [a] | 0 | 74 | 26 | 0 |
| P350-10-1 | 359 | 11.8 | 10 | 73 | 25 | 2 |
| P350-10-2 | 358 | 12.2 | 10 | 77 | 23 | 0 |
| P350-10-3 | 356 | 22.2 | 10 | 75 | 25 | 0 |
| P350-20 | 363 | 20.8 | 20 | 85 | 15 | 0 |

[a] Reactor pressure and temperature data lost.

## References

Bhaskar, T., Sera, A., Muto, A., Sakata, Y., 2008. Hydrothermal upgrading of wood biomass: influence of the addition of $K_2CO_3$ and cellulose/lignin ratio. Fuel 87, 2236–2242.

Cantero, D., Bermejo, M., Cocero, M., 2013. Kinetic analysis of cellulose depolymerization reactions in near critical water. J. Supercrit. Fluids 75, 48–57.

Cheng, S., D'cruz, I., Wang, M., Leitch, M., Xu, C., 2010. Highly efficient liquefaction of woody biomass in hot-compressed alcohol–water co-solvents. Energy Fuels 24, 4659–4667.

Demirbaş, A., 2000. Mechanisms of liquefaction and pyrolysis reactions of biomass. Energy Convers. Manag. 41, 633–646.

Di Blasi, C., 2008. Modeling chemical and physical processes of wood and biomass pyrolysis. Prog. Energy Combust. Sci. 34, 47–90.

Goudriaan, F., Peferoen, D., 1990. Liquid fuels from biomass via a hydrothermal process. Chem. Eng. Sci. 45 (8), 2729–2734.

Hashaikeh, R., Fang, Z., Butler, I., Hawari, J., Kozinski, J., 2007. Hydrothermal dissolution of willow in hot compressed water as a model for biomass conversion. Fuel 86, 1614–1622.

Karagöz, S., Bhaskar, T., Muto, A., Sakata, Y., Uddin, M., 2004. Low-temperature hydrothermal treatment of biomass: effect of reaction parameters on products and boiling point distributions. Energy Fuels 18, 234–241.

Knežević, D., vanSwaaij, W., Kersten, S., 2010. Hydrothermal conversion of biomass. II. Conversion of wood, pyrolysis oil, and glucose in hot compressed water. Ind. Eng. Chem. Res. 49, 104–112.

Kobayashi, N., Okada, N., Hirakawa, A., Sato, T., Kobayashi, J., Hatano, S., Itaya, Y., Mori, S., 2009. Characteristics of solid residues obtained from hot-compressed-water treatment of woody biomass. Ind. Eng. Chem. Res. 48, 373–379.

Liu, H.-M., Xie, X.-A., Li, M.-F., Sun, R.-C., 2012. Hydrothermal liquefaction of cypress: effects of reaction conditions on 5-lump distribution and composition. J. Anal. Appl. Pyrolysis 94, 177–183.

Minowa, T., Ogi, T., Dote, Y., Yokoyama, S.-Y., 1994. Effect of lignin content on the direct liquefaction of bark. Int. Chem. Eng. 34 (3), 428–430.

Modell, M., 1985. Gasification and liquefaction of forest products in supercritical water. In: Fundamentals of Thermochemical Biomass Conversion, Elsevier, Amsterdam, pp. 95–119 (Chapter 6).

Mosteiro-Romero, M., Vogel, F., Wokaun, A. Liquefaction of wood in hot compressed water: Part 2 — modeling of particle dissolution. Chemical Engineering Science, this issue, http://dx.doi.org/10.1016/j.ces.2013.12.039.

Müller, J., 2012. Hydrothermal Gasification of Biomass — Investigation on Coke Formation and Continuous Salt Separation with Pure Substrates and Real Biomass (Ph.D. thesis). ETH Zürich.

Müller, J., Vogel, F., 2012. Tar and coke formation during hydrothermal processing of glycerol and glucose. Influence of temperature, residence time and feed concentration. J. Supercrit. Fluids 70, 126–136.

Pińkowska, H., Wolak, P., Złocińska, A., 2012. Hydrothermal decomposition of alkali lignin in sub- and supercritical water. Chem. Eng. J. 187, 410–414.

Qu, Y., Wei, X., Zhong, C., 2003. Experimental study on the direct liquefaction of *Cunninghamia lanceolata* in water. Energy 28, 597–606.

Saisu, M., Sato, T., Watanabe, M., Aschiri, T., Arai, K., 2003. Conversion of lignin with supercritical water–phenol mixtures. Energy Fuels 17, 922–928.

Sun, P., Heng, M., Sun, S., Chen, J., 2010. Direct liquefaction of paulownia in hot compressed water: influence of catalysts. Energy 35, 5421–5429.

Toor, S., Rosendahl, L., Rudolf, A., 2011. Hydrothermal liquefaction of biomass: a review of subcritical water technologies. Energy 36, 2328–2342.

Vogel, F., Waldner, M., Rouff, A., Rabe, S., 2007. Synthetic natural gas from biomass by catalytic conversion in supercritical water. Green Chem. 9, 616–619.

Waldner, M., 2007. Catalytic Hydrothermal Gasification of Biomass for the Production of Synthetic Natural Gas (Ph.D. thesis). ETH Zürich.

Waldner, M., Vogel, F., 2005. Renewable production of methane from woody biomass by catalytic hydrothermal gasification. Ind. Eng. Chem. Res. 44, 4543–4551.

Xu, C., Lad, N., 2008. Production of heavy oils with high caloric values by direct liquefaction of woody biomass in sub/near-critical water. Energy Fuels 22 (1), 635–642.

Yáñez, R., Romaní, A., Garrote, G., Alonso, J., Parajó, J., 2009. Processing of *Acacia dealbata* in aqueous media: first step of a wood biorefinery. Ind. Eng. Chem. Res. 48, 6618–6626.

Yan, W., Hastings, J., Acharjee, T., Coronella, C., Vásquez, V., 2010. Mass and energy balances of wet torrefaction of lignocellulosic biomass. Energy Fuels 24 (9), 4738–4742.

Yu, Y., Lou, X., Wu, H., 2008. Some recent advances in hydrolysis of biomass in hot-compressed water and its comparisons with other hydrolysis methods. Energy Fuels 22, 46–60.

Zhang, B., von Keitz, M., Valentas, K., 2008. Thermal effects on hydrothermal biomass liquefaction. Biotechnol. Fuels Chem. 147, 143–150.

Zhong, C., Wei, X., 2004. A comparative experimental study on the liquefaction of wood. Energy 29, 1731–1741.